9 and 10 and the isotropic shifts of +19.94 and -3.88 ppm are applicable to this chelate, the fractions X_9 and X_{10} will be derived on the basis of observed isotropic shifts for H^B and H^C from the sets of equations of (1) and (3) and of (2) and (3). These lead

$$X_9(+19.94) + X_{10}(-3.88) = +14.26 \quad (1)$$

$$X_9(-3.88) + X_{10}(19.94) = -3.08 \quad (2)$$

$$X_9 + X_{10} = 1.0 \quad (3)$$

to values of 0.76 and 0.96 for X_9. On the other hand, the magnitudes of the isotropic shifts of H^I and H^J and the separation between them are almost the same as those of the *meso*-ptn chelate. The estimation of the distribution based on the isotropic shift of H^B seems to overestimate the contribution of **10**. The methine proton, H^A, shows almost the same isotropic shift as that of the *meso*-ptn chelate, and it is concluded that the bn chelate takes exclusively the conformation of **9**.

This view is supported further by the ^{13}C NMR spectrum. The isotropic shift of +66.1 ppm for the methyl carbon is almost the same as that of +62.6 ppm for $[Fe(CN)_4(meso\text{-ptn})]^-$.

$[Fe(CN)_4(R\text{-ptn})]^-$. Three signals appeared in both the ^1H and ^{13}C NMR spectra. These numbers of signals can be accounted for either by a rapid interconversion of the chelate rings among **11-13** or a predominant λ-skew-boat conformation, **12**, which belongs to C_2 symmetry. But the rapid interconversion is reasonably assumed to take place for the Fe(II) chelate. The isotropic shift of 2.09 ppm for $H^C + H^D$ is the middle point between that of -3.88 ppm for H^A of $[Fe(CN)_4(meso\text{-ptn})]^-$ and that of 8.03 ppm for the mean of $H^A + H^B$ of $[Fe(CN)_4(tn)]^-$. This suggests that the contribution from the axial proton exceeds that from the equatorial proton. Both protons are located in axial position in the conformer of **12**, but one of the two protons takes an axial position in the conformers of **11** and **14**. On the basis of estimated isotropic shifts for the axial and equatorial protons on C^1, eq 4

$$X_{12}(-3.88) + (1 - X_{12})(19.94 - 3.88)/2 = 2.09 \quad (4)$$

is derived, where the fraction of **12** is X_{12} and that of **11** and **14** are $(1 - X_{12})/2$. This equation leads to a value of 0.50 for X_{12}. The ratio of 50:50 for λ-skew-boat and chair forms is almost the same as that reported for $Ni(OH_2)_4(rac\text{-ptn})^{2+}$, i.e. 54:46.[18]

The isotropic shift for the methylene protons ($H^I + H^J$) is also smaller (-17.03 ppm) compared with the mean of those (-22.38 ppm) for the corresponding protons of $[Fe(CN)_4(meso\text{-ptn})]^-$.

The isotropic shift of +46.5 ppm for the methyl carbons of $[Fe(CN)_4(R\text{-ptn})]^-$ is considerably smaller than those for the bn and *meso*-ptn chelates, 66.1 and 62.6 ppm. For the latter two, methyl groups are oriented equatorially with the chelate ring with chair conformations. The smaller isotropic shift will be due to the axial orientation of one of the methyl groups in both of the chair conformers.

Acknowledgment. This work was supported by Grant-in-Aid for Scientific Research No. 546195 from the Ministry of Education, Science, and Culture of Japan. The authors wish to thank Drs. Ajioka and Yano of the University of Tokyo for providing us with 1,3-diaminobutane.

Registry No. $Na_2[Fe(CN)_4(tn)]$, 101403-91-2; $Na_2[Fe(CN)_4(bn)]$, 101403-92-3; $Na_2[Fe(CN)_4(meso\text{-ptn})]$, 101403-93-4; $Na_2[Fe(CN)_4(R\text{-ptn})]$, 101470-35-3; $Na[Fe(CN)_4(tn)]$, 101403-94-5; $H[Fe(CN)_4(tn)]$, 101403-95-6; $H[Fe(CN)_4(bn)]$, 101403-96-7; $H[Fe(CN)_4(meso\text{-ptn})]$, 101403-97-8; $H[Fe(CN)_4(R\text{-ptn})]$, 101470-36-4.

Supplementary Material Available: Figure 2, infrared spectra (Nujol mulls) of $H[Fe(CN)_4(tn)]\cdot 2H_2O\cdot(CH_3)_2CHOH$ (top) and $Na[Fe(CN)_4(tn)]\cdot 1.5H_2O$ (bottom) (1 page). Ordering information is given on any current masthead page.

Contribution from the Department of Applied Chemistry, Faculty of Engineering, Osaka University, Yamada-oka 2-1, Suita, Osaka 565, Japan

Multielectron Reductions of Alkyl Azides with $[Mo_2Fe_6S_8(SPh)_9]^{3-}$ and $[Mo_2Fe_6S_8(\mu\text{-}SEt)_3(SCH_2CH_2OH)_6]^{3-}$ in Homogeneous Systems and with a $(n\text{-}Bu_4N)_3[Mo_2Fe_6S_8(SPh)_9]$ Modified Glassy-Carbon Electrode in H_2O

Susumu Kuwabata, Koji Tanaka, and Toshio Tanaka*

Received September 26, 1985

The electrochemical behaviors of a $(n\text{-}Bu_4N)_3[Mo_2Fe_6S_8(SPh)_9]$ modified glassy-carbon electrode ([Mo-Fe]/GC) have been studied in water. The [Mo-Fe]/GC works stably in water and undergoes the two-electron-redox reaction arising from a $[Mo_2Fe_6S_8(SPh)_9]^{3-/5-}$ couple. The electrochemical reductions of $HOCH_2CH_2N_3$ (or CH_3N_3) not only by the [Mo-Fe]/GC in water at -1.25 V vs. SCE but also by $[Mo_2Fe_6S_8(SPh)_9]^{3-}$ and $[Mo_2Fe_6S_8(\mu\text{-}SEt)_3(SCH_2CH_2OH)_6]^{3-}$ dissolved in MeOH/THF (1:1 v/v) and in H_2O, respectively, with an Hg electrode at the same potential were carried out in order to compare the catalytic activity toward a multielectron reduction. In these systems, ammonia and hydrazine were formed for the first time as eight- and six-electron-reduction products of alkyl azide, respectively, together with the formation of $HOCH_2CH_2NH_2$ (or CH_3NH_2) and N_2 as two-electron-reduction products. The turnover number for the formation of NH_3 based on the amount of the cluster in the reduction with the [Mo-Fe]/GC attains 12000 in 2 h, which is much larger than that (a maximum of 3.5) obtained in the latter. The reaction is initiated with the displacement of a terminal thiolate ligand of the reduced cluster by $HOCH_2CH_2N_3$, affording the 1:1 adduct, followed by successive two-electron reductions of $HOCH_2CH_2N_3$.

Introduction

It is well-known that dinitrogen molecules coordinated to Mo and W in low oxidation states are reduced by acid stepwise to afford N_2H_4 and NH_3 in compensation for an increase in the oxidation states of the central metal atoms, and various azenide and hydrazide complexes have been isolated as reaction intermediates.[1-11] In this connection, electrochemical reduction of a hydrazide-molybdenum complex under dinitrogen has been proposed with the intention of regeneration of dinitrogen complexes, producing N_2H_4 or NH_3.[12] However such a catalytic

(1) Chatt, J.; Heath, G. A.; Richards, R. L. *J. Chem. Soc., Dalton Trans.* **1974**, 2074.
(2) Chatt, J.; Pearman, A. J.; Richards, R. L. *Nature (London)* **1975**, *253*, 39.
(3) Chatt, J.; Pearman, A. J.; Richards, R. L. *J. Organomet. Chem.* **1975**, *101*, C45.
(4) Chatt, J.; Pearman, A. J.; Richards, R. L. *J. Chem. Soc., Dalton Trans.* **1977**, 1853.
(5) Chatt, J.; Pearman, A. J.; Richards, R. L. *J. Chem. Soc., Dalton Trans.* **1977**, 2139.
(6) Chatt, J.; Richards, R. L. *J. Less-Common Met.* **1977**, *54*, 477.
(7) Heath, G. A.; Mason, R.; Thomas, K. M. *J. Am. Chem. Soc.* **1974**, *96*, 259.
(8) Hidai, M.; Kodama, T.; Sato, M.; Harakawa, M.; Uchida, Y. *Inorg. Chem.* **1976**, *15*, 2694.
(9) Day, V. W.; George, T. A.; Iske, S. D. A.; Wagner S. D. *J. Organomet. Chem.* **1976**, *112*, C55.
(10) Marsh, F. C.; Mason, R.; Thomas, K. M. *J. Organomet. Chem.* **1975**, *96*, C43.
(11) Mtunzi, S. D.; Richards, R. L. *J. Chem. Soc., Dalton Trans.* **1984**, 1329.

0020-1669/86/1325-1691$01.50/0

reduction of N_2 has not succeeded so far. This is in striking contrast to the smooth reduction of N_2 by nitrogenases in the presence of MgATP and $Na_2S_2O_4$.

Model systems developed by Schrauzer et al., who used aqueous solutions containing an oxomolybdenum(IV) complex and $NaBH_4$ or $Na_2S_2O_4$ as a reducing agent, can reduce very small amounts of various nitrogenase substrates.[13] Such systems, however, mimic a behavior of nitrogenases in some aspects, since the reduction of nitrogenase substrates has been enhanced by the addition of ATP and $[Fe_4S_4(SPh)_4]^{2-}$.[13b,14,15] These additives are supposed to activate molybdenum, facilitating the electron transfer from a reductant to molybdenum. The reduction of N_2 by those systems has been considered to proceed via N_2H_2, followed by its disproportionation to afford N_2H_4 and N_2, the former of which is further reduced to NH_3, as suggested from kinetic measurements and overall stoichiometry.[13b,15] The amount of NH_3 formed in the reduction of N_2, however, is very small.

On the other hand, Holm et al. have shown that $[Fe_4S_4(SPh)_4]^{3-}$ prepared by the reduction of $[Fe_4S_4(SPh)_4]^{2-}$ with sodium acenaphthylenide ($NaC_{12}H_8$) can reduce C_2H_2 to C_2H_4 and *cis*-$C_2D_2H_2$ selectively in the presence of CH_3COOH and CH_3COOD, respectively, in *N*-methylpyrrolidone in 60% yields.[16] Recently, we have demonstrated that $[Fe_4S_4(SPh)_4]^{2-}$ and $[Mo_2Fe_6S_8(SPh)_9]^{3-}$ function as catalysts for the reductions of C_2H_2, both in MeOH/THF and in H_2O,[17] and of C_2D_2 in H_2O (pH 6.0)[18] under controlled-potential electrolysis, giving C_2H_4 and *cis*-$C_2D_2H_2$, respectively. Thus, those clusters simulate well the behavior of nitrogenases with respect to the reduction of acetylene, since any side reactions such as the formation of C_2H_6 and C_4H_6 are practically inhibited under those conditions. Moreover, CH_3NC and CH_3CN undergo catalytic multielectron reductions[19] at the triple bonds by the reduced species of those clusters.[20] It seems, therefore, to be of interest to elucidate the catalytic activity of the clusters toward multielectron reductions in more detail, since nitrogenases reduce N_2 to NH_3 with eight electrons, as expressed by eq 1.[21,22] Along this line, the reduction of RN_3 by reduced

$$N_2 + 8H^+ + 8e^- \rightarrow 2NH_3 + H_2 \qquad (1)$$

species of metal clusters is of particular interest from the viewpoint that the two-electron reduction of RN_3 gives an equal amount of RNH_2 and N_2,[23] of which the latter may be concentrated around the clusters, possibly leading to a smooth reduction of N_2. This paper describes the multielectron reduction of RN_3 (R = CH_3, $HOCH_2CH_2$) directed toward the construction of nitrogenase model systems by using $[Mo_2Fe_6S_8X_3Y_6]^{3-}$ (X = Y = SPh; X = μ-SEt and Y = SCH_2CH_2OH) dissolved in MeOH/THF or in H_2O, and $(n\text{-}Bu_4N)_3[Mo_2Fe_6S_8(SPh)_9]$ modified on a glassy-carbon electrode in H_2O.

Experimental Section

Materials. Commercially available guaranteed reagent grades of LiCl, NaOH, H_3PO_4, and $HOCH_2CH{=}CH_2$ were used without further purification. Molybdenum–iron–sulfur clusters $(n\text{-}Bu_4N)_3[Mo_2Fe_6S_8(SPh)_9]$ ($(n\text{-}Bu_4N)_3$[Mo-Fe])[24,25] and $(Et_4N)_3[Mo_2Fe_6S_8(\mu\text{-}SEt)_3(SCH_2CH_2OH)_6]$ ($(Et_4N)_3$[Mo-Fe-OH])[26] and RN_3 (R = CH_3,[27] $HOCH_2CH_2$[28]) were prepared according to the literature method. Solvents used in this study were purified by distillation: CH_3OH from methoxide, THF from NaOH and then freshly cut sodium, DMF from CaH_2 under reduced pressure, and CH_3CN from P_2O_5. All solvents were redistilled and stored under N_2. Immediately before use they were bubbled with He gas for 1 h to remove dinitrogen dissolved in the solvents.

Preparation of a $(n\text{-}Bu_4N)_3$[Mo-Fe] Modified Glassy-Carbon Electrode. Glassy-carbon plates with areas of 1.0 and 3.0 cm^2 (Tokai Carbon Co. Ltd., SC-2) were polished with Al_2O_3 (0.3 μm) and washed with distilled water several times. Electrical lead copper wires were attached with silver–epoxy to the back of the polished glassy-carbon plate, and then the back and round rims of the glassy carbon plate were coated with epoxy resin. An acetonitrile solution of $(n\text{-}Bu_4N)_3$[Mo-Fe] ($1.0 \times 10^{-5} \sim 2.0 \times 10^{-3}$ mol dm^{-3}) was dropped on a polished surface of the glassy-carbon plates by a syringe technique and dried for ca.30 min under a dry N_2 stream. $(n\text{-}Bu_4N)_3$[Mo-Fe] modified glassy-carbon electrodes ([Mo-Fe]/GC) with surface areas of 1.0 and 3.0 cm^2 thus prepared were used for electrochemical measurements and the reduction of $HOCH_2CH_2N_3$, respectively. A rotating-ring disk-electrode (RRDE) technique was used in order to detect PhS^- liberated from $(n\text{-}Bu_4N)_3$[Mo-Fe] in solution. A glassy-carbon ring (7-mm outside diameter, 5-mm inside diameter, 8-mm length; Tokai Carbon Co. Ltd., P-5-100) was attached with epoxy resin around a glassy-carbon disk electrode (3-mm diameter) mounted in a glass tube (5-mm diameter; Yanagimoto MGF. Co. Ltd., GC-P2). An electrical lead copper wire was attached to the back of the ring glassy carbon with silver–epoxy and epoxy resin. This electrode was mounted in a glass tube with epoxy resin. The disk electrode was modified with $(n\text{-}Bu_4N)_3$[Mo-Fe] in the same way as described above. The RRDE was used at 1000 rpm by a rotating electrode head (Yanagimoto MFG. Co. Ltd., P10-RE).

Physical Measurements. Electronic absorption spectra were measured with a Union SM-401 spectrophotometer. Spectroelectrochemical experiments were carried out by the use of an optically transparent thin-layer electrode (OTTLE),[29] consisting of a Pt-gauze electrode in a 0.5-mm quartz cuvette, a Pt-wire auxiliary electrode, and a saturated calomel reference electrode (SCE). Electrochemical measurements of [Mo-Fe]/GC were carried out in a Pyrex cell equipped with a Pt auxiliary electrode, an SCE, and a nozzle for bubbling N_2 or He. Cyclic voltammograms, cathodic polarization, and RRDE curves were obtained by the use of a Hokuto Denko HB-401 potentiostat, a Hokuto Denko HB-107A function generator, and a Yokogawa Electric Inc. 3077 X-Y recorder.

Reduction of Alkyl Azide. The reductions of alkyl azide by the electrochemically reduced species of [Mo-Fe]$^{3-}$ in MeOH/THF (1:1 v/v) and of [Mo-Fe-OH]$^{3-}$ in water were carried out under a controlled-potential electrolysis condition (−1.25 V vs. SCE) with an electrolysis cell. The cell consisted of three compartments: one for an Hg working electrode, the second for a platinum auxiliary electrode that was separated from the Hg electrode by a cation-exchange membrane (Nafion film), and the third for a SCE reference electrode. The volume of these compartments were 45, 30, and 10 cm^3, respectively, and the former two were connected to volumetric flasks with stainless-steel tubes (i.d. = 0.4 mm).

After a stream of He was passed through the electrolysis cell and the volumetric flasks for 30 min to displace the air, a MeOH/THF (1:1 v/v) solution containing $(n\text{-}Bu_4N)_3$[Mo-Fe], CH_3N_3, and LiCl or an aqueous solution containing $(Et_4N)_3$[Mo-Fe-OH], $HOCH_2CH_2N_3$, and H_3PO_4/NaOH buffer was introduced into the electrode compartments by a syringe technique. Then the electrolysis cell was placed in a thermostat at 30 °C, and the solution in the cell was stirred magnetically for 1 h. The reduction of alkyl azides was started by applying the electrolysis potential to the Hg working electrode with a potentiostat.[30] The reduction of $HOCH_2CH_2N_3$ by [Mo-Fe]/GC in water containing $HOCH_2CH_2N_3$ and H_3PO_4/NaOH as a supporting electrolyte was carried out in a similar way. The charge consumed in the reduction of alkyl azides was measured with a Hokuto Denko HF-201 coulometer.

Product Analysis. The volume of the gas evolved in the reduction (H_2 and N_2) was determined from the change of the meniscus of water in a

(12) Pickett, C. J.; Leigh, G. J. *J. Chem. Soc., Chem. Commun.* **1981**, 1033.
(13) (a) Schrauzer, G. N.; Doemeny, P. A. *J. Am. Chem. Soc.* **1971**, *93*, 1608. (b) Schrauzer, G. N.; Keifer, G. W.; Tano, K.; Doemeny, P. A. *J. Am. Chem. Soc.* **1974**, *96*, 641. (c) Robinson, P. R.; Moorehead, E. L.; Weathers, B. J.; Ufkes, E. A.; Vickrey, T. M.; Schrauzer, G. N. *J. Am. Chem. Soc.* **1977**, *99*, 3657. (d) Hughes, L. A.; Hui, L. N.; Schrauzer, G. N. *Organometallics* **1983**, *2*, 486 and references therein.
(14) Tano, K.; Schrauzer, G. N. *J. Am. Chem. Soc.* **1975**, *97*, 5404.
(15) Schrauzer, G. N.; Robinson, P. R.; Moorehead, E. L.; Vickrey, T. M. *J. Am. Chem. Soc.* **1976**, *98*, 2815.
(16) McMillan, R. S.; Renaud, J.; Reynolds, J. G.; Holm, R. H. *J. Inorg. Biochem.* **1979**, *11*, 213.
(17) Tanaka, K.; Honjo, M.; Tanaka, T. *J. Inorg. Biochem.* **1984**, *22*, 1873.
(18) Tanaka, K.; Tanaka, M.; Tanaka, T. *Chem. Lett.* **1981**, 185.
(19) Defined as successive two-electron reductions in this paper.
(20) Tanaka, K.; Imasaka, Y.; Tanaka, M.; Honjo, M.; Tanaka, T. *J. Am. Chem. Soc.* **1982**, *104*, 4258.
(21) Smith, B. E.; Lowe, D. J.; Bray, R. C. *J. Biochem.* **1972**, *130*, 641.
(22) Smith, B. E.; Lowe, D. J.; Bray, R. C. *J. Biochem.* **1973**, *135*, 331.
(23) Iversew, P. E. *Encyclopedia of Electrochemistry of the Elements*; Marcel Dekker: New York, 1979; Vol. XIII, p 209.
(24) Christou, G.; Garner, C. D. *J. Chem. Soc., Dalton, Trans.* **1980**, 2354.
(25) Christou, G.; Garner, C. D.; Miller, R. M. *J. Chem. Soc., Dalton. Trans.* **1980**, 2363.
(26) Palermo, R. E.; Power, P. P.; Holm, R. H. *Inorg. Chem.* **1982**, *21*, 173.
(27) Forster, M. O.; Fierz, H. E. *J. Chem. Soc.* **1908**, *93*, 1865.
(28) Pimroth, O.; Wislicenus, W. *Ber. Dtsch. Chem. Ges.* **1905**, *38*, 1573.
(29) Lexa, D.; Savent, J. M.; Zickler, J. *J. Am. Chem. Soc.* **1977**, *99*, 2786.
(30) Detailed description about a electrolysis cell was shown in a previous paper.[17]

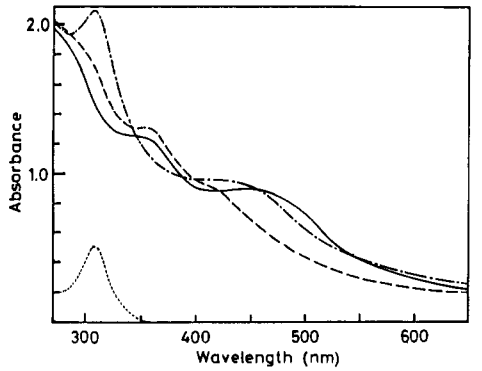

Figure 1. Electronic absorption spectra of $(n\text{-}Bu_4N)_3$[Mo-Fe] (5.0×10^{-4} mol dm^{-3}) (—), the reduced species produced at −1.10 V (vs. SCE) in the absence (– –) and presence (–·–) of CH_3N_3 (5.0×10^{-3} mol dm^{-3}), and the PhS^- anion (- -) formed by the reduction of PhSH (5.0×10^{-4} mol dm^{-3}) at −1.50 V (vs. SCE) in DMF.

volumetric flask connected to the working electrode cell. At a fixed interval 0.1-cm^3 portions were sampled with a pressure-lock syringe (Precision Sampling) from the gaseous phases not only in the working electrode cell but also in the volumetric flask through septum caps attached to the top of the flasks. Gas analysis was performed on a Shimadzu gas chromatograph GC-4B with a 2-m column filled with 13x molecular sieves at 70 °C using He (40 cm^3/min) as a carrier gas.

The analysis of a reactant (alkyl azide) and products (alkylamine, hydrazine, and ammonia) in solution was performed at a fixed time interval by sampling 0.1-cm^3 portions of the solutions in the working electrode cell with syringe techniques through a septum cap. In order to liberate free alkylamine and ammonia in the solutions taken from the cell, 0.1 cm^3 of the solution was mixed with an aqueous NaOH solution (ca. 30 wt %, 1×10^{-3} cm^3) in a sealed tube with a septum cap. Then, the resulting alkaline solution was analyzed with Shimadzu GC-7A and GC-6A gas chromatographs with a 1.6-m column filled with PEG-HT 5% and KOH 1% Uniport HP 60/80 (for the determination of alkyl azide and alkylamine) and with a 1.0-m column filled with Chromsorb 103 (for the determination of NH_3), respectively. The amount of N_2H_4 in the solution was determined by spectrophotometric titration.[31]

Results and Discussion

Interaction of $[Mo\text{-}Fe]^{3-}$ with CH_3N_3. Holm et al. have prepared a variety of Mo–Fe–S clusters as models of the active sites in nitrogenases,[32] of which a single cubane Mo–Fe cluster forms stable 1:1 adducts with various bases including some nitrogenases substrates such as N_3^- and CH_3CN.[32g,h] On the other hand, a double cubane Mo–Fe–S cluster $[Mo_2Fe_6S_8(SPh)_9]^{3-}$ ($[Mo\text{-}Fe]^{3-}$) with coordinatively saturated molybdenum has not been reported to form such adducts. The terminal thiophenolate ligands bonded to Fe atoms, however, are expected to undergo substitution by other bases, while the bridging thiophenolate ligands are inert to substitution reactions.[33] The electronic absorption spectrum of $[Mo\text{-}Fe]^{3-}$ in organic solvents shows a change upon electrochemical reduction followed by reoxidation.[34] The interaction of CH_3N_3 not only with $[Mo\text{-}Fe]^{3-}$ but also with the reduced forms can, therefore, easily be examined by means of spectroelectrochemical techniques. The electronic absorption spectrum of $(n\text{-}Bu_4N)_3$[Mo-Fe] (λ_{max} = 360 and 450 nm; a solid line in Figure 1) in DMF does not change at all upon addition of CH_3N_3 into the solution, suggesting that essentially no interaction occurs between CH_3N_3 and $[Mo\text{-}Fe]^{3-}$. The controlled-potential electrolysis of $(n\text{-}Bu_4N)_3$[Mo-Fe] at −1.10 V[35] in the presence of CH_3N_3 in DMF results in a shift of the 470-nm band to 440 nm accompanied by the appearance of a new band at 306 nm, as shown by a dotted broken line in Figure 1, which is markedly different from the spectrum of $[Mo\text{-}Fe]^{4-}$ (a broken line in Figure 1) prepared under controlled-potential electrolysis at −1.10 V in the absence of CH_3N_3. The 306-nm band observed only in the reduced species of $[Mo\text{-}Fe]^{3-}$ in the presence of CH_3N_3 may be associated with the PhS^- anion liberated from the cluster, since the band position and the feature coincide with those in the spectrum of PhS^- prepared by the electrochemical reduction of PhSH at −1.50 V[36] in DMF (a dotted line in Figure 1). In addition, the absorptivity at 306 nm in the spectrum of $[Mo\text{-}Fe]^{4-}$ in the presence of CH_3N_3 indicates that 1 mol of PhS^- (ϵ_M = 19 800 mol^{-1} dm^3 cm^{-1}) dissociates from 1 mol of the cluster. One molecule of CH_3N_3 may, therefore, substitute a terminal PhS^- ligand of $[Mo\text{-}Fe]^{4-}$. The CH_3N_3–cluster adduct thus formed can easily be reoxidized by electrolysis at −0.6 V vs. SCE in DMF to bring about an immediate decrease in the absorbance at 306 nm down to about 10%; the final spectrum obtained after 1 h was almost consistent with that of $[Mo\text{-}Fe]^{3-}$. The electrochemical reduction–oxidation cycle of $[Mo\text{-}Fe]^{3-}$ in the presence of CH_3N_3 may, therefore, be expressed by eq 2.

$$[Mo_2Fe_6S_8(SPh)_9]^{3-} \underset{-e^-}{\overset{+e^-}{\rightleftharpoons}} [Mo_2Fe_6S_8(SPh)_9]^{4-} \underset{-CH_3N_3}{\overset{+CH_3N_3}{\rightleftharpoons}} [Mo_2Fe_6S_8(SPh)_8CH_3N_3]^{3-} + SPh^- \quad (2)$$

Cyclic Voltammogram of [Mo-Fe]/GC in Water. The cyclic voltammogram (CV) of [Mo-Fe]/GC in the range −0.5 to −1.7 V (vs. SCE) in water (pH 10) is depicted by line a in Figure 2, which shows that a cathodic current due to the reduction of protons by the reduced species of $[Mo\text{-}Fe]^{3-}$ begins to flow at a negative potential slightly greater than −1.1 V.[37] This is consistent with the fact that $[Mo\text{-}Fe]^{5-}$ reacts with protons to evolve H_2 in DMF.[38] The area of a broad but well-defined anodic wave observed around −0.7 V (vs. SCE) in the anodic scan depends on the amount of the cluster modified on the glassy-carbon electrode, while the peak potential has not been changed at all. The charge consumed in the anodic wave[39] was determined as 5.8 mC when 3.0×10^{-8} mol

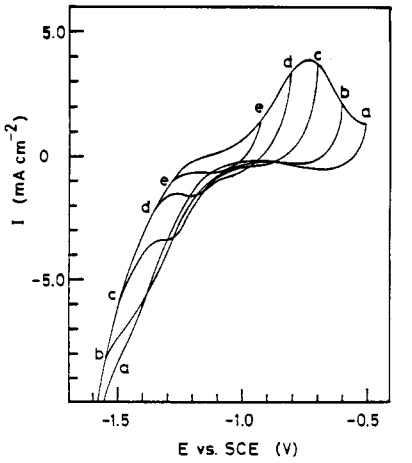

Figure 2. Cyclic voltammograms of [Mo-Fe]/GC in an aqueous H_3PO_4/NaOH buffer (0.2 mol dm^{-3}) solution (pH 10). Anodic switching potentisl (V): (a) −0.5; (b) −0.6; (c) −0.7; (d) −0.8; (e) −0.9. dE/dt = 100 mV s^{-1}.

(31) Watt, G. W.; Chrips, J. *Anal. Chem.* **1952**, *24*, 2066.
(32) (a) Averill, B. A.; Herskovitz, T.; Holm, R. H.; Ibers, J. A. *J. Am. Chem. Soc.* **1973**, *95*, 3523. (b) Laune, R. W.; Ibers, J. A.; Frankel, R. B.; Papaefthymiou, G. C.; Holm, R. H. *J. Am. Chem. Soc.* **1977**, *99*, 84. (c) Wolff, T. E.; Berg, J. M.; Hodgson, K. O.; Frankel, R. B.; Holm, R. H. *J. Am. Chem. Soc.* **1979**, *101*, 4140. (d) Wolff, T. E.; Power, P. P.; Frankel, R. B.; Holm, R. H. *J. Am. Chem. Soc.* **1980**, *102*, 4694. (e) Armstrong, W. H.; Holm, R. H. *J. Am. Chem. Soc.* **1981**, *103*, 6246. (f) Christou, G.; Sabat, M.; Ibers, J. A.; Holm, R. H. *Inorg. Chem.* **1982**, *21*, 3518. (g) Palermo, R. E.; Holm, R. H. *J. Am. Chem. Soc.* **1983**, *105*, 4310. (h) Palermo, R. E.; Singh, R.; Bashkin, J. K.; Holm, R. H. *J. Am. Chem. Soc.* **1984**, *106*, 2600 and references therein.
(33) Palermo, R. E.; Power, P. P.; Holm, R. H. *Inorg. Chem.* **1982**, *21*, 173.
(34) Christou, G.; Mascharak, P. K.; Armstrong, W. H.; Papaefthymiou, G. C.; Frankel, R. B.; Holm, R. H. *J. Am. Chem. Soc.* **1982**, *104*, 2820.
(35) This potential is sufficiently negative for the reduction of $[Mo\text{-}Fe]^{3-}$ to $[Mo\text{-}Fe]^{4-}$; see ref 34.
(36) Bradbury, J. R.; Hanson, G. R.; Boyd, I. W.; Gheller, S. F.; Wedd, A. G.; Murry, K. S.; Bond, A. M. *Proceedings of the Third International Conference on the Chemistry and Uses of Molybdenum*; Climax Molybdenum: Ann Arbor, MI, 1979; p 300.
(37) H_2 evolution by the glassy carbon electrode not modified with $(n\text{-}Bu_4N)_3$[Mo-Fe] occurred at a potential more negative than −1.8 V (vs. SCE) at pH 10.
(38) Yamamura, T.; Christou, G.; Holm, R. H. *Inorg. Chem.* **1983**, *22*, 939.

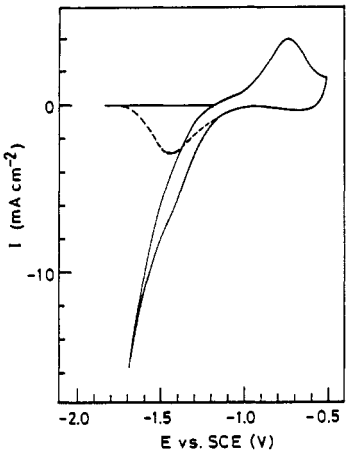

Figure 3. Cyclic voltammogram of [Mo-Fe]/GC (—) and the calculated cathodic wave (- -) obtained by subtracting the current in cathodic scan from that in an anodic scan of [Mo-Fe]/GC between −1.2 and −1.7 V (vs. SCE).

of $(n\text{-}Bu_4N)_3$[Mo-Fe] was modified on the 1.0-cm^2 glassy-carbon electrode. Thus, the anodic wave can be assigned to the two-electron-oxidation process from $[Mo\text{-}Fe]^{5-}$ to $[Mo\text{-}Fe]^{3-}$ by comparison with the CV of $[Mo\text{-}Fe]^{3-}$ in DMF.[40] The cathodic wave coupled with the anodic wave around −0.7 V may, therefore, be concealed in the cathodic current due to H_2 evolution. In fact, when the CV is taken by changing only anodic switching potentials from −0.5 to −0.9 V at a 0.1-V interval with the constant cathodic potential at −1.7 V (lines a–e in Figure 2, respectively), a weak cathodic wave appears as a shoulder in the cathodic current due to H_2 evolution and continuously shifts to more anodic potentials. A decrease in the peak current accompanied by the anodic shift of the cathodic wave (a > b > c > d > e in Figure 2) may be explained by a decrease in the amount of $[Mo\text{-}Fe]^{3-}$ formed by the oxidation of $[Mo\text{-}Fe]^{5-}$ on the glassy-carbon electrode upon the cathodic shift of the anodic switching potential.

It should be noted that there has been found no hysteresis between the cathodic and the anodic sweeps in the CV of lines b–e at the more negative potential than the potentials where their I–E curves in those cathodic sweeps coincide with that of line a in the anodic sweep. Thus, the wave at the potentials more cathodic than −1.1 V is associated with H_2 evolution on the reduced species $[Mo\text{-}Fe]^{5-}$ prepared electrochemically on a glassy-carbon electrode. The current difference between the cathodic and anodic scans of line a in Figure 2 in the range −1.1 to −1.7 V may, therefore, correspond to the number of charges consumed by reduction of the cluster. In fact, the cathodic wave calculated from the difference between the currents in the cathodic and anodic scans gives a well-defined wave centered around −1.5 V, and the feature is fairly similar to that of the anodic wave around −0.7 V as depicted by a broken line in Figure 3. Furthermore, a multiscanning CV of [Mo-Fe]/GC for 2 h reveals that a decrease in the peak current of the anodic wave around −0.7 V was less than 5% compared with that in the first sweep. Thus, $[Mo\text{-}Fe]^{3-}$ modified on a glassy-carbon electrode works stably in water to undergo a two-electron-redox reaction.

Cyclic Voltammogram of [Mo-Fe]/GC in the Presence of $HOCH_2CH_2N_3$. The first sweep CV of [Mo-Fe]/GC in the presence of $HOCH_2CH_2N_3$ in water (pH 10) (a broken line in Figure 4) is essentially consistent with that in the absence of the substrate in water (pH 10). Repeated scans conducted in the range −0.5 to −1.7 V, however, resulted in a gradual anodic shift of the threshold potential of the cathodic current accompanied by a decrease in the peak current of the anodic wave around −0.7 V, and the change of the CV almost ceased within 10 cycles (a solid line in Figure 4). This result suggests that [Mo-Fe]/GC is

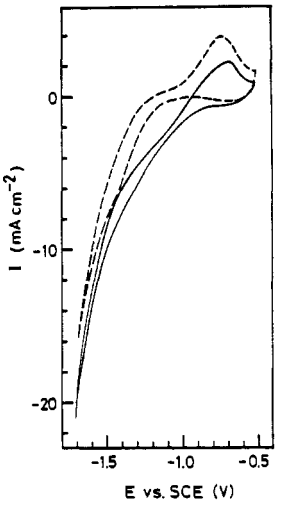

Figure 4. First (- -) and tenth (—) scannings in the cyclic voltammograms of [Mo-Fe]/GC in an aqueous H_3PO_4/NaOH buffer (0.2 mol dm^{-3}) solution (pH 10) containing $HOCH_2CH_2N_3$ (1×10^{-2} mol dm^{-3}). dE/dt = 100 mV s^{-1}.

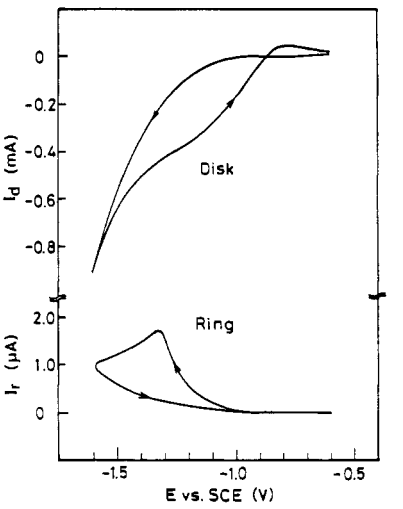

Figure 5. Current curves of the disk and ring electrodes vs. potentials of the disk electrode modified with $(n\text{-}Bu_4N)_3$[Mo-Fe] (4×10^{-9} mol) in an aqueous H_3PO_4/NaOH buffer solution (0.2 mol dm^{-3}) containing $HOCH_2CH_2N_3$ (1×10^{-2} mol dm^{-3}). The potential of the ring electrode was 0.4 V, dE/dT = 10 mV s^{-1}, and ω = 1000 rpm.

completely activated toward the reduction of $HOCH_2CH_2N_3$[41] in that period since the CV (a solid line) was not changed for another 1 h of multiscanning. In addition, the [Mo-Fe]/GC electrode in water (pH 10), which had been removed from the aqueous $HOCH_2CH_2N_3$ solution after multiscanning for 1 h followed by washing with O_2-free distilled water, gave a CV almost identical with that shown in Figure 3. Thus, the [Mo-Fe]/GC is not decomposed during the reduction of $HOCH_2CH_2N_3$.

The process of the activation of [Mo-Fe]/GC toward the reduction of $HOCH_2CH_2N_3$ was further investigated by the use of a rotating-ring disk electrode (RRDE) whose disk moiety was modified by $(n\text{-}Bu_4N)_3$[Mo-Fe]. The I_d–E_d curve (I_d and E_d represent the current and the potential at the disk electrode, respectively) in the presence of $HOCH_2CH_2N_3$ (10 mmol dm^{-3}) in water (pH 10) exhibits an appreciable increase in the I_d value in the anodic sweep compared with that in the cathodic one even in the first potential sweep under the rotation of the RRDE at 1000 rpm, as shown in Figure 5. On the other hand, when the E_d value is shifted more cathodically than −1.0 V, the ring electrode being maintained at E_r = +0.4 V (vs. SCE) (E_r, ring electrode

(39) Facci, J.; Murray, R. W. *Anal. Chem.* **1982**, *54*, 772.
(40) $[Mo\text{-}Fe]^{3-}$ in DMF undergoes two successive redox reactions of the 3−/4− and 4−/5− couples at −1.02 and −1.23 V (vs. SCE), respectively.
(41) The reduction of $HOCH_2CH_2N_3$ by a glassy-carbon electrode not modified with $(n\text{-}Bu_4N)_3$[Mo-Fe] has not occurred at a potential more positive than −1.50 V (vs. SCE) in water at pH 10.

Table I. Reduction of RN_3 (R = $HOCH_2CH_2$, CH_3) Catalyzed by $[Mo\text{-}Fe]^{3-}$ or $[Mo\text{-}Fe\text{-}OH]^{3-}$ under Electrolysis at −1.25 V vs. SCE

cluster[a]	solvent[b]	t/min	substrate	mol of product/mol of cluster				
				H_2	N_2	RNH_2	NH_3	N_2H_4
$[Mo\text{-}Fe\text{-}OH]^{3-}$	H_2O, pH 9	80	$HOC_2H_4N_3$[c]	14	7.8	9.1	3.5	0.05
$[Mo\text{-}Fe\text{-}OH]^{3-}$	H_2O, pH 11	80	$HOC_2H_4N_3$[c]	10	7.8	9.1	2.6	0.02
$[Mo\text{-}Fe\text{-}OH]^{3-}$	H_2O, pH 13	120	$HOC_2H_4N_3$[c]	0	10.0	8.5	1.3	0.10
$[Mo\text{-}Fe]^{3-}$	CH_3OH/THF (1:1)[d]	230	CH_3N_3[e]	1.8	9.8	10.8	1.8	0.13

[a] 8.0×10^{-4} mol dm^{-3}. [b] $HSCH_2CH_2OH$ (4.0×10^{-3} mol dm^{-3}) was added in order to stabilize the cluster in an H_3PO_4/NaOH buffer solution (14 dm^3). [c] Initial concentration was 8.0×10^{-3} mol dm^{-3}. [d] LiCl (0.24 mol dm^{-3}) was added as a supporting electrolyte. [e] Initial concentration was 8.7×10^{-3} mol dm^{-3}.

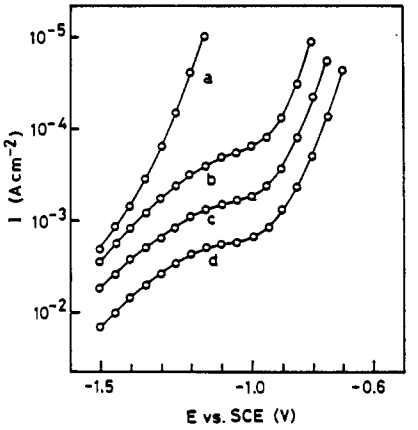

Figure 6. Cathodic polarizations of $(n\text{-}Bu_4N)_3[Mo\text{-}Fe]$ (2.0×10^{-9} mol) modified on a glassy-carbon electrode in an aqueous H_3PO_4 NaOH buffer (0.2 mol dm^{-3}) solution (pH 10) containing $HOCH_2CH_2N_3$ with the following concentrations (mol dm^{-3}): (a) 0; (b) 5.0×10^{-3}; (c) 1.0×10^{-2}; (d) 2.0×10^{-2}.

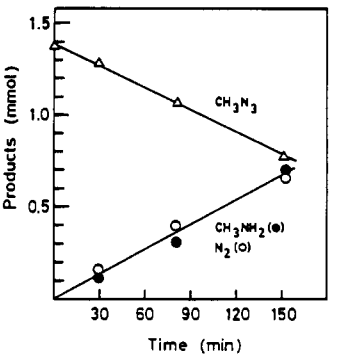

Figure 7. Reduction of CH_3N_3 catalyzed by $[Mo\text{-}Fe]^{3-}$ (8.0×10^{-4} mol dm^{-3}) under electrolysis at −1.25 V vs. SCE in MeOH/THF (1:1 v/v, 20 cm^3). The initial concentration of CH_3N_3 was 6.6×10^{-2} mol dm^{-3}.

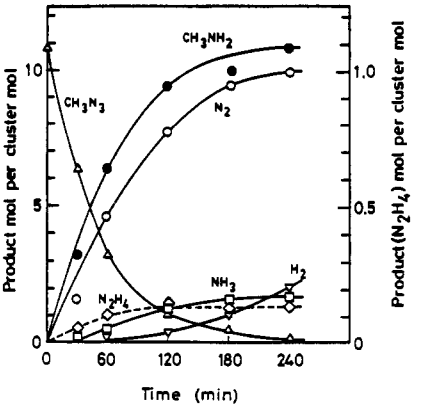

Figure 8. Reduction of CH_3N_3 catalyzed by $(n\text{-}Bu_4N)_3[Mo\text{-}Fe]$ (8.0×10^{-4} mol dm^{-3}) under electrolysis at −1.25 V vs. SCE in MeOH/THF (1:1 v/v, 20 cm^3). The initial concentration of CH_3N_3 was 8.7×10^{-3} mol dm^{-3}.

potential), an anodic ring current, I_r, is detected, which reaches a maximum at $E_d = -1.3$ V and thereafter decreases. The I_r has been detected neither in the second sweep of the E_d nor upon the E_r being shifted to a value more negative than 0 V. The oxidation behavior on the ring electrode is completely consistent with that of PhSH in water at pH 10. Thus, the substitution reaction of PhS^- in $[Mo\text{-}Fe]^{3-}$ modified on the disk electrode by $HOCH_2CH_2N_3$ takes place during the first cyclic sweep of the E_d value when the RRDE rotates at 1000 rpm. Moreover, after the second cyclic sweep, the I_d–E_d curves obtained in the cathodic and the anodic directions not only no longer showed hysteresis but also coincided with that in the first anodic sweep of Figure 5. The activation of [Mo-Fe]/GC toward the reduction of $HOCH_2CH_2N_3$, therefore, is caused by the dissociation of PhS^- from the cluster.

Cathodic polarizations of [Mo-Fe]/GC were examined in the presence of various concentrations of $HOCH_2CH_2N_3$ in water (pH 10) in order to obtain further information on the reduction of $HOCH_2CH_2N_3$ by [Mo-Fe]/GC. The increase in the cathodic current at potentials more negative than −1.1 V in the absence of $HOCH_2CH_2N_3$ (curve a in Figure 6) is due to the reduction of a proton by [Mo-Fe]/GC as described above. The I–E plots of [Mo-Fe]/GC in the presence of $HOCH_2CH_2N_3$ shift anodically, and the magnitude of shifts is proportional to the concentrations of $HOCH_2CH_2N_3$ (curves b–d in Figure 6), suggesting that [Mo-Fe]/GC can effectively reduce $HOCH_2CH_2N_3$. The gentle slopes of the I–E plots between −1.0 and −1.1 V in the presence of $HOCH_2CH_2N_3$ may, therefore, be due to limiting currents of the reduction of $HOCH_2CH_2N_3$. On the other hand, the increase in the cathodic currents at potentials more negative than −1.1 V may result from the reductions of protons together with $HOCH_2CH_2N_3$.

Reductions of CH_3N_3 and $HOCH_2CH_2N_3$ in Homogeneous Systems. In order to compare the catalytic activity of $[Mo\text{-}Fe]^{3-}$ modified on a glassy-carbon electrode with those of $[Mo\text{-}Fe]^{3-}$ and $[Mo\text{-}Fe\text{-}OH]^{3-}$ in homogeneous systems, the reduction of RN_3 (R = CH_3, $HOCH_2CH_2$) by $(n\text{-}Bu_4N)_3[Mo\text{-}Fe]$ and $(Et_4N)_3[Mo\text{-}Fe\text{-}OH]$ was carried out in MeOH/THF and H_2O, respectively, under the electrolysis conditions. As shown in Figure 7, the reduction of CH_3N_3 under controlled-potential electrolysis at −1.25 V (vs. SCE) with an Hg working electrode in MeOH/THF (1:1 v/v, 20 cm^3) containing $(n\text{-}Bu_4N)_3[Mo\text{-}Fe]$ (8.0×10^{-4} mol dm^{-3}), CH_3N_3 (6.6×10^{-2} mol dm^{-3}), and LiCl (0.24 mol dm^{-3}) produces an equal amount of CH_3NH_2 and N_2 without evolving H_2. The current efficiency for the formation of CH_3NH_2 was nearly 100%, suggesting that almost all the electrons transferred from the electrode to the cluster are consumed in the two-electron reduction of CH_3N_3 (eq 3). When the

$$CH_3N_3 + 2H^+ + 2e^- \rightarrow CH_3NH_2 + N_2 \quad (3)$$

concentration of CH_3N_3 is less than 1.0×10^{-2} mol dm^{-3}, however, the amount of N_2 produced in the reduction is less than that of CH_3NH_2, and small amounts of N_2H_4 (eq 4) and NH_3 (eq 5) are

$$CH_3N_3 + 6H^+ + 6e^- \rightarrow CH_3NH_2 + N_2H_4 \quad (4)$$

$$CH_3N_3 + 8H^+ + 8e^- \rightarrow CH_3NH_2 + 2NH_3 \quad (5)$$

formed by the six- and eight-electron reductions of CH_3N_3, respectively, accompanied by H_2 evolution, as shown in Figure 8 and Table I. The amount of N_2H_4 formed increases for the initial 120 min and thereafter remains almost constant, whereas the formation of NH_3 with an induction period still continues to increase in amount with time (Figure 8), indicating that the

Table II. Reduction of $HOCH_2CH_2N_3$ Catalyzed by a $(n\text{-}Bu_4N)_3$[Mo-Fe] (4.2×10^{-9} mol) Modified Glassy-Carbon Electrode (3.0 cm^2) in Aqueous Solution

amt of $HOC_2H_4N_3$[a]/ μmol	E vs. SCE/V	pH	t/min	mol of product/mol of cluster				
				H_2	N_2	$HOC_2H_4NH_2$	NH_3	N_2H_4
50	−1.25	10	120	3.8×10^3	1.1×10^4	1.2×10^4	2.3×10^3	0.9×10^2
100	−1.25	10	120	7.3×10^3	2.1×10^4	2.3×10^4	4.4×10^3	1.6×10^2
300	−1.25	10	120	2.5×10^4	6.4×10^4	7.1×10^4	1.2×10^4	5.1×10^2
100	−1.25	7	120	1.5×10^5	1.8×10^4	2.1×10^4	6.4×10^3	5.2×10^2
100	−1.25	12	120	0	2.3×10^4	2.4×10^4	1.8×10^3	0
100	−1.10	10	240	0	2.3×10^4	2.3×10^4	0	0
100[b]	−1.25	10	120	8.1×10^3	2.3×10^4	2.4×10^4	0	0

[a] In a 0.2 mol dm^{-3} H_3PO_4/NaOH buffer solution (20 cm^3). [b] $HOCH_2CH{=}CH_2$ (0.1 mol dm^{-3}) was added.

reduction of CH_3N_3 to NH_3 proceeds via N_2H_4 as an intermediate. This is consistent with the recent report that N_2H_4 can be reduced to NH_3 by the same cluster under electrolysis at −1.25 V in MeOH/THF with a current efficiency of almost 100%.[42]

Quite similarly, the reduction of $HOCH_2CH_2N_3$ by $(Et_4N)_3$[Mo-Fe-OH] (8.0×10^{-4} mol dm^{-3}) in H_2O (pH 9, 11, and 13) under electrolysis at −1.25 V produced NH_3 and N_2H_4 together with $HOCH_2CH_2NH_2$ and N_2 when the concentration of $HOCH_2CH_2N_3$ was less than 1.0×10^{-2} mol dm^{-3}. The representative results also are summarized in Table I. The amount of N_2H_4 formed in aqueous solutions increased only for the initial 60 min and then attained a constant concentration. Thus, the reductions of CH_3N_3 and $HOCH_2CH_2N_3$ by $[Mo\text{-}Fe]^{3-}$ in MeOH/THF and by $[Mo\text{-}Fe\text{-}OH]^{3-}$ in water, respectively, may proceed by the same mechanism.

It has been proposed that nitrogenases reduce N_2 to afford NH_3 via N_2H_2 and N_2H_4 as intermediates. Although the existence of neither free nor enzyme-bound N_2H_2 has so far been identified in the reduction of N_2 by nitrogenase because of its instability at room temperature, the formation of N_2H_4 has been detected on treating the enzyme with an aqueous acidic or an alkaline solution while it was functioning under dinitrogen.[43] In addition, Schrauzer et al. have demonstrated that the presence of olefins in their model systems of N_2 fixation by oxomolybdenum complexes completely depresses the formation not only of N_2H_4 but also of NH_3 owing to an effective trapping of N_2H_2, which may be formed as an intermediate.[13b] In the present study on the reduction of $HOCH_2CH_2N_3$ (1.0×10^{-2} mol dm^{-3}) by $(Et_4N)_3$[Mo-Fe-OH] (8.0×10^{-4} mol dm^{-3}) in water (pH 10) in the presence of allyl alcohol (0.1 mol dm^{-3}) and of CH_3N_3 (8.0×10^{-3} mol dm^{-3}) by $(n\text{-}Bu_4N)_3$[Mo-Fe] (8.0×10^{-4} mol dm^{-3}) in a C_2H_4-saturated MeOH/THF solution as well, only $HOCH_2CH_2NH_2$ and CH_3NH_2, respectively, together with N_2 and H_2, were produced; neither NH_3 nor N_2H_4 has been detected in the reaction mixtures. This result suggests that the present reduction of RN_3 (R = $HOCH_2CH_2$ and CH_3) proceeds via an N_2H_2 intermediate as a four-electron-reduction product of RN_3, giving N_2H_4 and NH_3 successively, since allyl alcohol and C_2H_4 react neither with N_2H_4 nor with NH_3.

Reduction of $HOCH_2CH_2N_3$ by [Mo-Fe]/GC. In view of the low yields for the production of NH_3 in the reduction of RN_3 in homogeneous systems (Table I), there may hardly occur effective electron transfer from the electrode to the cluster for the reduction of RN_3 with eight electrons. This is probably because only the cluster on the electrode surface can accept additional electrons from the electrode to proceed with such a multielectron reduction. This difficulty may be overcome by the use of [Mo-Fe]/GC in place of the cluster dissolved in solvents; the reduction of $HOCH_2CH_2N_3$ with [Mo-Fe]/GC under electrolysis at −1.25 V in an aqueous solution produces N_2H_4 and NH_3 effectively without any induction periods as well as $HOCH_2CH_2NH_2$ and N_2 even for the initial azide concentration of 1.5×10^{-2} mol dm^{-3}, as shown in Figure 9. It should be mentioned that neither NH_3, N_2H_4, nor H_2 has been formed in the presence of such a high concentration of the azide in homogeneous systems. The amount of N_2H_4 formed increases with time for the initial 30 min and thereafter remains essentially constant. It is worth noting that the turnover nubmer for the formation of NH_3, based on the amount of the cluster modified on a glassy-carbon electrode, is improved tremendously and attains more than 1×10^4 for 2 h.

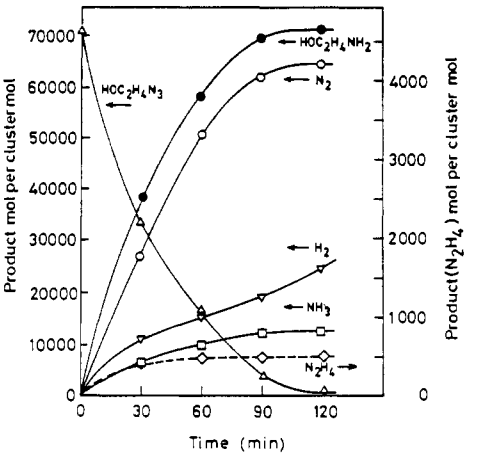

Figure 9. Reduction of $HOCH_2CH_2N_3$ catalyzed by a $(n\text{-}Bu_4N)_3$[Mo-Fe] (4.2×10^{-9} mol) modified glassy-carbon electrode under electrolysis at −1.25 V vs. SCE in an aqueous H_3PO_4/NaOH buffer (0.2 mol dm^{-3}) solution (pH 10; 20 cm^3).

The amount of the cluster modified on the glassy-carbon electrode largely influences the rate of the reduction of $HOCH_2CH_2N_3$ as shown in Figure 10, which indicates that the maximum rate with respect to the formation of either reduction product is obtained in the $(1.4\text{–}2.2) \times 10^{-9}$ mol cm^{-2} $(n\text{-}Bu_4N)_3$[Mo-Fe] range, whose amounts correspond to a few layered clusters on the glassy-carbon electrode under the assumption that the cluster occupies ca. 1.3×10^{-14} cm^2/molecule.[44] The decrease in the rate of the reduction with an increase in the amounts of the cluster modified (more than 2.2×10^{-9} mol cm^{-2}) may be due to lowering the conductivity of the electrode. On the other hand, the steep decrease in the rate at less than 1.4×10^{-9} mol/cm^2 of the cluster may result from an insufficient coating of the glassy-carbon electrode with the cluster. The typical results for the reduction of $HOCH_2CH_2N_3$ by [Mo-Fe]/GC are summarized in Table II, which reveals that the amount of NH_3 produced is proportional to the initial concentrations of $HOCH_2CH_2N_3$,[45] in contrast to the reduction in homogeneous systems. Thus, the [Mo-Fe]/GC used in this study can effectively be used for the multielectron reduction of $HOCH_2CH_2N_3$. As expected from the proton concentration, the amount of H_2 produced decreases with an increase in the pH value. The current efficiency for the formation of NH_3,

(42) Hozumi, Y.; Imasaka, Y.; Tanaka, K.; Tanaka, T. *Chem. Lett.* **1983**, 897.
(43) Thorneley, R. N. F.; Eady, R. R.; Lowe, D. J. *Nature (London)* **1978**, *272*, 557.
(44) Wolff, T. E.; Berg, J. M.; Hodgson, K. O.; Frankel, R. B.; Holm, R. H. *J. Am. Chem. Soc.* **1979**, *101*, 4140.
(45) For a concentration of more than 50 μmol cm^{-3} of $HOCH_2CH_2N_3$, NH_3 was produced without an induction period, but a large cathodic current (more than 50 mA cm^{-2}) accompanied with vigorous N_2 evolution tore the cluster coating on the glassy carbon, resulting in a decrease of the reduction ability of the electrode with the passage of time.

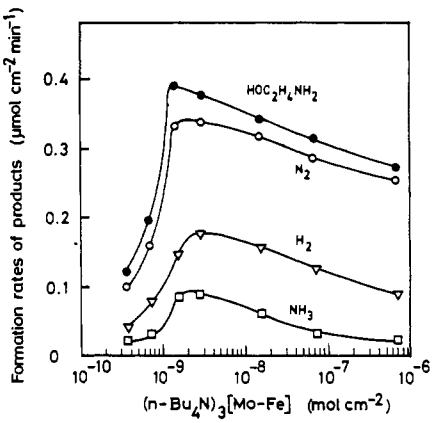

Figure 10. Dependence of the formation rate of products in the reduction of $HOCH_2CH_2N_3$ at −1.25 V vs. SCE on the amount of $(n\text{-}Bu_4N)_3$[Mo-Fe] modified on a glassy-carbon electrode in an aqueous H_3PO_4/NaOH buffer (0.2 mol dm^{-3}) solution (pH 10) containing $HOCH_2CH_2N_3$ (5.0×10^{-3} mol dm^{-3}).

therefore, increases with increasing pH value up to pH 12, where the cluster may be stable.

The reduction of $HOCH_2CH_2N_3$ (5.0×10^{-3} mol dm^{-3}) even with [Mo-Fe]/GC in the presence of allyl alcohol (0.1 mol dm^{-3}) in water under electrolysis at −1.25 V (vs. SCE) produces N_2 and $HOCH_2CH_2NH_2$ together with H_2, and neither NH_3 nor N_2H_4 has been formed at all, suggesting that N_2H_2 is involved as a reaction intermediate for the formation of N_2H_4 and NH_3 in the reduction of $HOCH_2CH_2N_3$ by [Mo-Fe]/GC.

The reduction of $HOCH_2CH_2N_3$ with [Mo-Fe]/GC under electrolysis at −1.10 V (vs. SCE) gave only $HOCH_2CH_2NH_2$ and N_2 without forming either NH_3, N_2H_4, or H_2. Thus, the anodic shift of the electrode potential from −1.25 to −1.10 V vs. SCE resulted in a decrease of the ability of the multielectron reduction of [Mo-Fe]/GC. Such a characteristic behavior of [Mo-Fe]/GC toward the reduction of alkyl azide can be explained from the cathodic polarization curves of the electrode (Figure 4); the limiting currents of [Mo-Fe]/GC observed between −1.0 and −1.1 V (vs. SCE) in the presence $HOCH_2CH_2N_3$ are, therefore, due to the two-electron reduction of $HOCH_2CH_2N_3$ and an increase of the current at more negative than −1.10 V (vs. SCE) results from the multielectron reduction of $HOCH_2CH_2N_3$ accompanied by H_2 evolution.

Registry No. $(Bu_4N)_3$[Mo-Fe], 68197-68-2; $(Et_4N)_3$[Mo-Fe-OH], 79466-71-0; $[Mo\text{-}Fe]^{3-}$, 68136-29-8; $[Mo\text{-}Fe]^{4-}$, 81276-61-1; $[Mo\text{-}Fe]^{5-}$, 76125-83-2; CH_3N_3, 624-90-8; $HOCH_2CH_2N_3$, 1517-05-1; H_2, 1333-74-0; N_2, 7727-37-9; NH_3, 7664-41-7; N_2H_4, 1333-74-0; CH_3NH_2, 74-89-5; $HOCH_2CH_2NH_2$, 141-43-5; carbon, 7440-44-0; allyl alcohol, 107-18-6.

Contribution from Inorganic Chemistry 1,
Chemical Center, University of Lund, S-221 00 Lund, Sweden

Electronic Absorption and Magnetic Circular Dichroism Spectra of Monomeric and Dimeric Platinum(II) and Palladium(II) Iodide Complexes

Lars-Fride Olsson

Received June 21, 1985

Magnetic circular dichroism (MCD) and absorption spectra of PdI_4^{2-}(aq) for $1/\lambda < 3.8$ μm^{-1} and of PtI_4^{2-} and $Pt_2I_6^{2-}$ for $1/\lambda < 5.0$ μm^{-1} in methanol and at −65 °C have been recorded. In the latter complexes, there is intense absorption ($\epsilon = 5 \times 10^4$ cm^{-1} M^{-1}) in the UV region and several bands have been detected. The well-established LMCT (ligand p to metal d) assignment for PdX_4^{2-} holds also for PdI_4^{2-} with singlet–triplet transitions included. The most plausible assignment for PtI_4^{2-} seems to be a combination of LMCT and internal metal d–p transitions. The vis/near-UV bands have been assigned as singlet–triplet transitions, the far-UV bands as the corresponding singlet–singlet d–p transitions, and the bands between these systems as LMCT transitions.

Introduction

For many years the electronic structures as revealed by the spectra and spectral assignments of square-planar (D_{4h}) d^8 complexes of platinum(II) and palladium(II) have attracted much attention. The first attempts[1] concentrated on the symmetry-forbidden d–d (ligand field) bands in $PtCl_4^{2-}$. The assignments were established from single-crystal[2] and magnetic circular dichroism (MCD) spectra.[2,3] When such measurements were extended to the symmetry-allowed bands in the UV region,[3,4] the results showed that different assignments must be given for $PtCl_4^{2-}$ and $PdCl_4^{2-}$. The two suggestions were ligand-to-metal charge transfer (LMCT) for the bands in $PdCl_4^{2-}$ but metal d to metal p charge transfer for at least one band in $PtCl_4^{2-}$ (this was first suggested by Chatt et al.[1] in their early study). That internal metal transitions (i.e. d to p) should occur at considerably lower energies in Pt as compared to Pd could be inferred from both atomic spectral data[4] and MO calculations.[5]

Unfortunately, the assignments for the chloride complexes are based on two high-intensity bands[6] only. There are only those two bands below the high-energy limit of commercial spectrophotometers (5.3 μm^{-1} or 185 nm). A possible way to increase the number of bands would be to substitute chloride by bromide[7] and iodide: the concomitant red shift would make more bands accessible. Thus, for $PtBr_4^{2-}$ Isci and Mason[7] found additional strong bands in the UV region that they assigned to a mixture of internal metal and LMCT transitions.

This work presents a similar study of PtI_4^{2-} and PdI_4^{2-}. These complexes are only stable in solutions containing a large excess of ligand[8,9] ($C_I \geq 0.5$ M); otherwise, disturbing reactions take place within a few seconds: solvolysis and precipitation take place in water (PtI_2, PdI_2) and formation of the dimer occurs especially in organic solvents ($Pt_2I_6^{2-}$ and its Pd analogue)

$$2PtI_4^{2-} \rightarrow Pt_2I_6^{2-} + 2I^- \quad (1)$$

Unfortunately, I^- has a very strong absorption in the UV region,[9] which prevents measurements above 3.8 μm^{-1} (260 nm). However, by a low-temperature technique, described elsewhere,[10] it has been possible to keep PtI_4^{2-} in solution without added I^- for the time needed to record its absorption and MCD spectra to 5.0 μm^{-1} (cf. Figure 3).

As expected, the spectra of the iodide complexes contain many more symmetry-allowed bands than those of the chloride complexes. This is not only due to the expected red shift; in the iodide

(1) Chatt, J.; Gamlen, G. A.; Orgel, L. E. *J. Chem. Soc.* **1958**, 486.
(2) Martin, D. S.; Lenhardt, C. A. *Inorg. Chem.* **1964**, *3*, 1368.
(3) McCaffery, A. J.; Schatz, P. N.; Stephens, P. J. *J. Am. Chem. Soc.* **1968**, *90*, 5730.
(4) Anex, B. G.; Takeuchi, N. *J. Am. Chem. Soc.* **1974**, *96*, 4411.
(5) Larsson, S.; Olsson, L. F.; Rosén, A. *Int. J. Quantum Chem.* **1984**, *25*, 201.
(6) Elding, L. I.; Olsson, L. F. *J. Phys. Chem.* **1978**, *82*, 69.
(7) Isci, H.; Mason, W. R. *Inorg. Chem.* **1984**, *23*, 1565.
(8) Corain, B.; Poë, A. J. *J. Chem. Soc. A* **1967**, 1318.
(9) Elding, L. I.; Olsson, L. F. *Inorg. Chem.* **1977**, *16*, 2789.
(10) Olsson, L. F. *Chem. Scr.* **1985**, *25*, 194.

0020-1669/86/1325-1697$01.50/0